Simulation of ion transport characteristics in a collisionless rf sheath

2005 J. Phys. D: Appl. Phys. 38 1899

(http://iopscience.iop.org/0022-3727/38/12/008)

INSTITUTE OF PHYSICS PUBLISHING JOURNAL OF PHYSICS D: APPLIED PHYSICS

J. Phys. D: Appl. Phys. **38** (2005) 1899–1904 doi:10.1088/0022-3727/38/12/008

Simulation of ion transport characteristics in a collisionless rf sheath

Zu-li Liu[1], Xing-bin Jing[1] and Kai-lun Yao[1,2]

[1] Department of Physics, Huazhong University of Science and Technology, Wuhan 430074, People's Republic of China

[2] International Center of Materials Physics, Chinese Academy of Science, Shenyang 110015, People's Republic of China

E-mail: zlliu@hust.edu.cn and jingxb1978@163.com

Received 25 January 2005, in final form 16 March 2005
Published 3 June 2005
Online at stacks.iop.org/JPhysD/38/1899

Abstract

With a self-consistent fluid model, we study the transport characteristics of the collisionless radio frequency (rf) sheath in a high density plasma and calculate the spatiotemporal ion density and the potential drop across the sheath in one rf cycle for an rf-bias frequency of 13.56 MHz. We also study the effects of the rf frequency on the voltage at the electrode, the sheath width, the ion energy distribution (IED) and the ion angular distribution (IAD) at the electrode. The simulated results indicate that the incidence angles of the ions impinging on the electrode are less than 8° when the ion velocity in the direction perpendicular to the sheath field is assumed to be a Boltzmann distribution. It is concluded that the rf frequency plays a crucial role for the energy and angular distributions of ions impinging on the electrode surface, and the IED and IAD are affected by the plasma density and the rf-bias power.

1. Introduction

For several decades, low pressure discharges have been used in the microelectronics industry for the fabrication and processing of thin films of metals, dielectrics and semiconducting materials. Many experimenters and theoreticians made efforts to understand and model the physical processes involved, especially the radio-frequency (rf) gas discharges [1, 4–9, 12]. As we know, the sheath plays a crucial role in controlling the movement of the charged particles towards the electrodes, though its width is only a few times that of the electronic Debye length λ_D in the quasi-neutral plasma region. Thus, it is important to study the spatiotemporal variations of the sheath width, the ion flux and the electric field across the rf sheath.

Many models [2–9] have been applied to obtain the characteristics of the charged particles in the plasma, particularly in the rf sheath [4–9]. Using the Monte Carlo method, Liu *et al* [2] studied the behaviour of electrons in the positive column of a helium dc gas discharge under the influence of a mirror magnetic field and a uniform electric field. In the step model of collisionless and collisional rf sheaths for high frequency reported by Lieberman [5, 6], the electron density was assumed to abruptly drop to zero at the sheath–plasma boundary. However, this assumption oversimplified the Poisson's equation. Recently, Edelberg and Aydil [7] and Dai *et al* [8] introduced the dynamic model of the rf sheath by the ion fluid equations coupled with an equivalent circuit model and simulated the ion energy distribution (IED) at the electrode.

The ion energy and angular distributions of the incident ions at various energies are very significant during the plasma etching processes. One may expect the IED to be affected by the modulation of the electric field in the rf sheath. Edelberg and Aydil [7] calculated the IED in a collisionless rf sheath using the Monte Carlo method, but they did not simulate the ion angle distribution. Kawamura *et al* [9] made a detailed analysis of the IED in the rf sheath while the ion angular distribution (IAD) at the electrode was simply described. According to the collisionless sheath model, Raja and Linne [10] and Gottscho [11] investigated the IAD functions (IADFs), bombarding the electrode surface in a low pressure and high density plasma while the IADFs were calculated by analytic models.

In this paper, using a self-consistent fluid model of the collisionless rf sheath, we calculate the voltage at the electrode, the sheath width, the potential drop and the ion density across the sheath. The IED and IAD arriving at the electrode are also simulated. The outline of this paper is as follows. In section 2,

we present the basic model of the rf sheath including the sheath equations, equivalent circuit model, boundary conditions and the methods for calculating the IED and IAD. In section 3, the potential drop and the ion density across the sheath, and the IED and IAD at the electrode with various rf-bias frequencies are shown. The effects of variable plasma density and of variable rf-bias power on the IED and IAD incident on the electrode are also discussed. Finally, we draw some conclusions in section 4.

2. Model description

2.1. Sheath equations

For simplicity, we consider that the plasma consists of one species of cold ions and electrons with a uniform temperature. The working gas in the capacitance coupled rf discharge is argon. For the low pressure discharge, it is reasonable to neglect collisions between ions and neutral particles since the sheath width is much less than the mean free path of ions and neutral particles. The ion thermal motion can be neglected due to the ion temperature being much smaller than the directional kinetic energy in the sheath regions. Furthermore, the charged particles, the electrons and the ions, are absorbed completely by the vessel wall and the electrodes.

The one-dimensional sheath model is shown in figure 1, and the rf sheath is formed near one electrode surface. The electrode is placed at $z = 0$, and the plasma–sheath interface is at the position $z = d_{\mathrm{sh}}(t)$. The one-dimensional spatiotemporal variations of the ion density $n_{\mathrm{i}}(z, t)$ and drift velocity $u_{\mathrm{i}}(z, t)$ are described by the cold ion continuity and momentum balance equations:

$$\frac{\partial n_{\mathrm{i}}}{\partial t} + \frac{\partial}{\partial z}(n_{\mathrm{i}} u_{\mathrm{i}}) = 0, \tag{1}$$

$$m_{\mathrm{i}} \frac{\partial u_{\mathrm{i}}}{\partial t} + m_{\mathrm{i}} u_{\mathrm{i}} \frac{\partial u_{\mathrm{i}}}{\partial z} = -e \frac{\partial V}{\partial z}. \tag{2}$$

Here, m_{i}, n_{i}, u_{i}, are the mass, the ion density and the velocity of the ion, respectively, and e is the base unit of charge. The electrical potential $V(z, t)$ inside the sheath is given by Poisson's equation,

$$\frac{\partial^2 V}{\partial t^2} = -\frac{e}{\varepsilon_0}(n_{\mathrm{i}} - n_{\mathrm{e}}), \tag{3}$$

where ε_0 is the vacuum permittivity, and n_{e} is the electron density. Due to the electron oscillating frequency in the plasma being much higher than the typically applied rf frequency 13.56 MHz, the electrons respond to the changes in the instantaneous potential. When the potential at the plasma–sheath edge is selected to be the reference zero potential, the electron density is given by the Maxwell–Boltzmann distribution

$$n_{\mathrm{e}} = n_0 \exp\left(\frac{eV}{k_{\mathrm{B}} T_{\mathrm{e}}}\right). \tag{4}$$

Here, T_{e} is the electron temperature and n_0 is the electron density at the plasma–sheath boundary. According to the quasi-neutral condition in plasma, the electron density equals the plasma density n_{p} at $z = d_{\mathrm{sh}}(t)$, and k_{B} is the Boltzmann constant.

In order to solve equations (1)–(3) for the fluid model, we must choose suitable boundary conditions at the electrode surface and the plasma–sheath interface. We suppose that the ions enter the sheath from the plasma–sheath interface with a velocity equal to the Bohm velocity u_{B}; that is,

$$u_{\mathrm{i}} = u_{\mathrm{B}} = \sqrt{\frac{k_{\mathrm{B}} T_{\mathrm{e}}}{m_{\mathrm{i}}}}, \qquad \text{at } z = d_{\mathrm{sh}}(t), \tag{5}$$

where $d_{\mathrm{sh}}(t)$ is the time dependent sheath width. The ion density n_{i} at the plasma–sheath boundary equals the plasma density n_{p}:

$$n_{\mathrm{i}} = n_{\mathrm{p}}, \qquad \text{at } z = d_{\mathrm{sh}}(t). \tag{6}$$

Finally, the boundary conditions of the potential, which affect intensely the ions' action in the sheath, are expressed by

$$V = V_{\mathrm{e}}(t), \qquad \text{at } z = 0, \tag{7}$$

$$V = 0, \qquad \text{at } z = d_{\mathrm{sh}}(t). \tag{8}$$

Here, the instantaneous voltage $V_{\mathrm{e}}(t)$ can be obtained self-consistently by the equivalent circuit model [7, 8]. When the applied current at the electrode is sinusoidal, the current balance equation given by Edelberg and Aydil [7] is expressed as

$$I_{\mathrm{t}}(t) - I_{\mathrm{e}}(t) - I_{\mathrm{d}}(t) = I_{\max} \sin(2\pi f t), \tag{9}$$

where f is the applied rf frequency and $I_{\max}$ is the amplitude of the rf-bias current. The total ion current bombarding the electrode is derived as [8]

$$I_{\mathrm{t}}(t) = e u_{\mathrm{i}}(0, t) n_{\mathrm{i}}(0, t) A, \tag{10}$$

where A is the electrode area. The current through the diode represents the variation of the electron current as a function of the potential drop at the electrode, and is taken to be

$$I_{\mathrm{e}}(t) = \frac{e u_{\mathrm{e}} n_0 A}{4} \exp\left(\frac{e V_{\mathrm{e}}(t)}{k_{\mathrm{B}} T_{\mathrm{e}}}\right), \tag{11}$$

where $u_{\mathrm{e}} = \sqrt{8 k_{\mathrm{B}} T_{\mathrm{e}} / \pi m_{\mathrm{e}}}$ is the mean velocity of the electron mass m_{e}. The last term on the left of equation (9) denotes the capacitive displacement current, and it is given by [7]

$$I_{\mathrm{d}}(t) = \frac{\mathrm{d}Q}{\mathrm{d}t} = C_{\mathrm{sh}}(t) \frac{\mathrm{d}V_{\mathrm{e}}(t)}{\mathrm{d}t}. \tag{12}$$

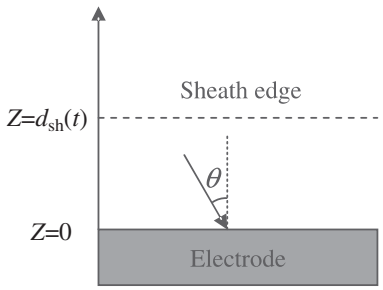

Figure 1. Schematic diagram of the rf sheath model near one electrode at some time. Here, $z = 0$ and $d_{\mathrm{sh}}(t)$ represent the origin of the one-dimensional coordinate and the plasma–sheath interface, respectively, and θ is the ion incidence angle at the electrode.

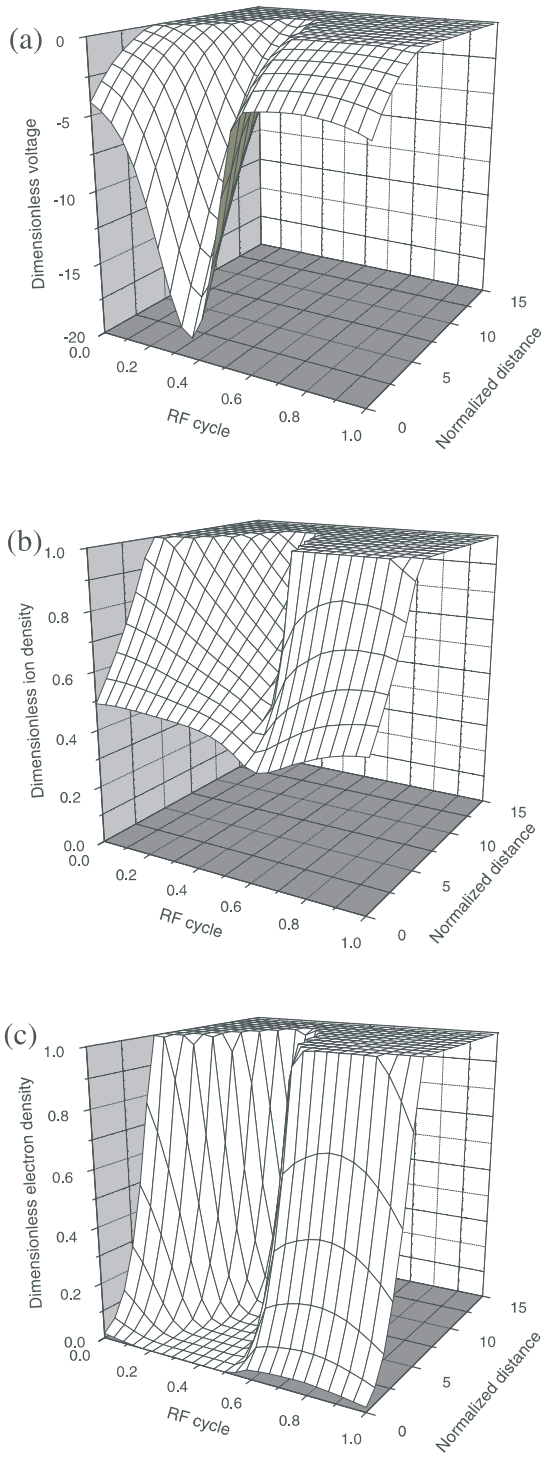

Figure 2. Spatiotemporal profiles of (*a*) the potential $V(z, t)$, (*b*) the ion density $n_i(z, t)$ and (*c*) the electron density $n_e(z, t)$ inside the sheath during one rf cycle. The rf frequency is 13.56 MHz, and the plasma density and the rf-bias power are 2.1×10^{11} cm^{-3} and 75 W, respectively.

Here, the time dependent sheath capacitance $C_{sh}(t)$ is expressed as

$$C_{sh}(t) = \frac{\varepsilon_0 A}{d_{sh}(t)}. \tag{13}$$

The current balance equation (9) can be solved using the fourth-order Runge–Kutta method, and the potential drop at the

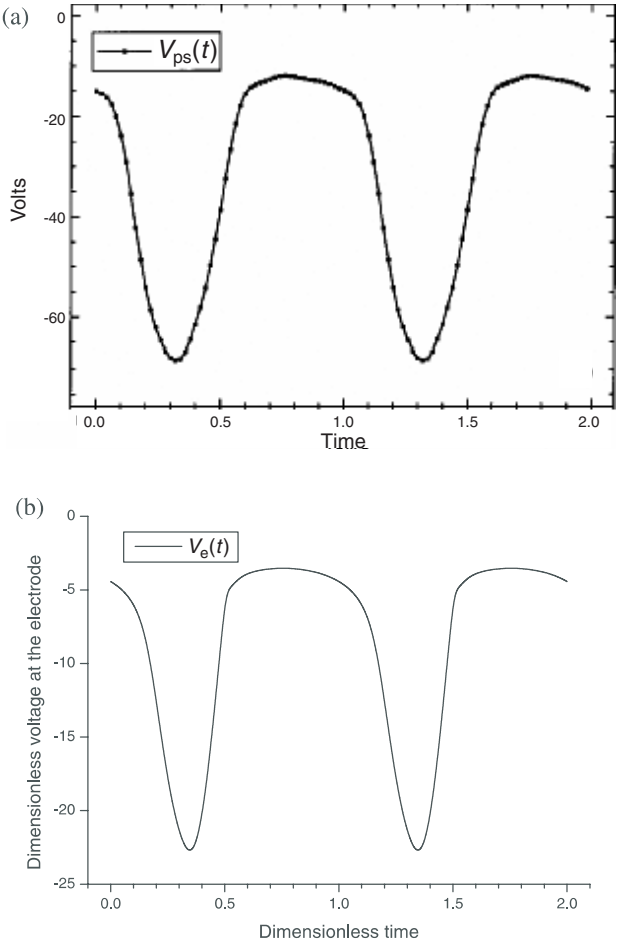

Figure 3. (*a*) An experimental wave form for the sheath voltage during two rf periods from [12]. The rf frequency, the rf-bias power and the pressure are 1.0 MHz, 8.0 W and 10 mTorr, respectively. (*b*) The simulated voltage at the electrode with the rf frequency, the rf-bias power and the plasma density are kept constant at 1.0 MHz, 9.7 W and 3.22×10^{10} cm^{-3}, respectively.

electrode, $V_e(t)$, can been obtained. Then, with the obtained voltage in the sheath, we solve the fluid equations and Poisson's equation using the second-order finite difference scheme in space and an explicit scheme in time. The iteration is repeated with the given accuracy until the potential and the sheath width as a function of time converge to a periodic steady-state solution.

2.2. IED and IAD

One may simulate directly the IED using the density $n_i(0, t)$ and the velocity $u_i(0, t)$ of the ions bombarding the electrode. This method is suitable for the collisionless sheath only. The IED can be calculated using [8]

$$f(\varepsilon) = \frac{\Delta N(\varepsilon)}{\Delta \varepsilon}. \tag{14}$$

Here, $\varepsilon = m_i u_i^2(0, t)/2$ is the ion energy arriving at the electrode and N is the ion number with a certain energy value.

To calculate the distribution of the ion angles striking the electrode, a simplified Monte Carlo model of the collisionless ion transport across the sheath is used. The model different

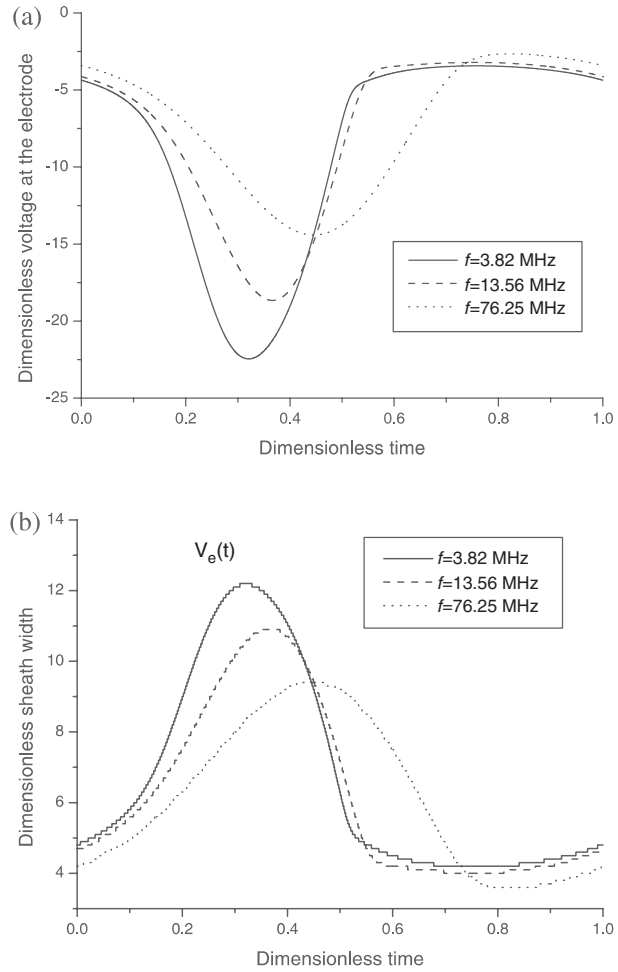

Figure 4. (*a*) The instantaneous electrode voltage and (*b*) the time dependent sheath width for several rf frequencies with the plasma density, the rf-bias power and the electron temperature are kept constant at $2.1 \times 10^{11}\,\mathrm{cm}^{-3}$, 75 W and 3 eV, respectively.

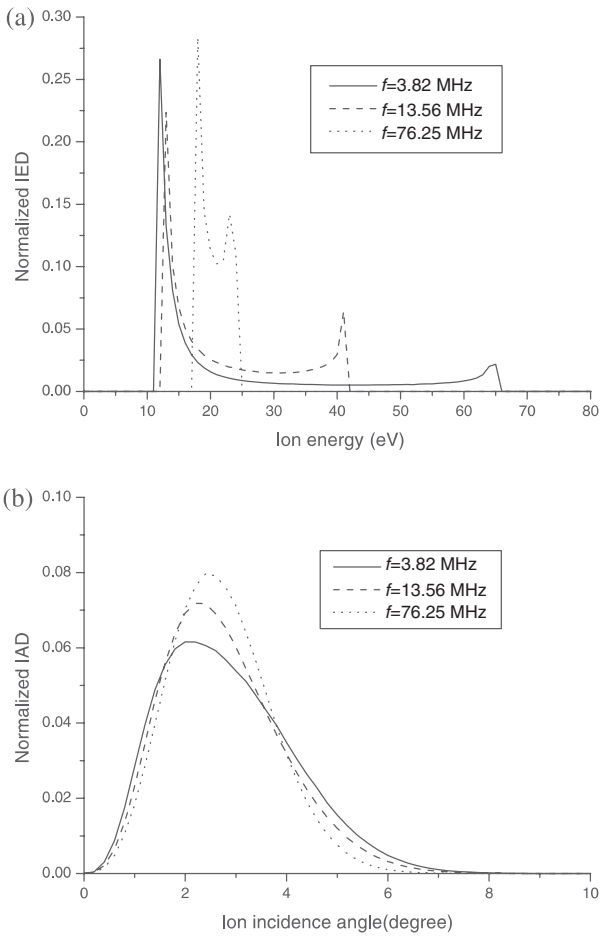

Figure 5. Effects of the rf frequency on (*a*) the IED and (*b*) the IAD impinging on the electrode for an Ar plasma. The ion temperature is fixed at 300 K. Other input parameters are the same as those in figure 4.

from the analytical model described by Gottscho [11] may be suitable only for a collisionless sheath. From section 2.1, we know that both the ion density and the ion velocity on the electrode at any time in one rf cycle can be obtained with the self-consistent fluid model of the sheath. Then, one can calculate the number N of ions incident on the electrode in one rf cycle with angle below a certain value. Thus, the IAD at the electrode can be expressed as

$$f(\theta) = \frac{\Delta N(\theta)}{\Delta \theta}. \tag{15}$$

Here, the ion incidence angle, $\theta = \arctan(u_\perp/u_\parallel)$, is defined as the angle between the ion velocity and the normal direction of the electrode surface. The velocity $u_\parallel$ of an ion in the direction parallel to the sheath field is obtained by the fluid model. The ion velocity $u_\perp$ perpendicular to the sheath field at the plasma–sheath boundary is picked randomly from a Maxwellian velocity distribution with temperature T_i, which is assumed to be 300 K.

$$f(u_\perp) = \sqrt{\frac{m_\mathrm{i}}{2\pi k_\mathrm{B} T_\mathrm{i}}} \exp\left(-\frac{m_\mathrm{i} u_\perp^2}{2k_\mathrm{B} T_\mathrm{i}}\right). \tag{16}$$

3. Results and discussion

In this section, we present some results by solving the current balance equation, the fluid equations and Poisson's equation. It is found that the IED and IAD are affected by the rf-bias frequency, the plasma density and the rf-bias power. In the simulation, the input parameters are $n_\mathrm{p} = 2.1 \times 10^{11}\,\mathrm{cm}^{-3}$, $k_\mathrm{B}T_\mathrm{e} = 3\,\mathrm{eV}$, $T_\mathrm{i} = 300\,\mathrm{K}$, $f = 13.56\,\mathrm{MHz}$, $A = 325\,\mathrm{cm}^2$. For convenience, we have used dimensionless forms for time, position, potential, ion velocity and density.

Figures 2(*a*)–(*c*) display the spatiotemporal variations of the voltage amplitude, the ion density and the electron density inside the sheath for an rf frequency of 13.56 MHz, plasma density of $2.1 \times 10^{11}\,\mathrm{cm}^{-3}$ and rf-bias power of 75 W. Figure 2(*a*) shows that the spatial variation of the potential alters significantly near the electrode and the temporal profile oscillates periodically with the rf time. Figure 2(*b*) shows that the ion density varies obviously with the spatial variable, but changes gently with time. In figure 2(*c*) one can see that the electron density changes obviously near the electrode within the distance of several Debye lengths.

In figure 3, we compare the numerical results of the sheath voltage with those [12] measured experimentally during two rf periods. In the simulation, the rf-bias frequency, the rf-bias

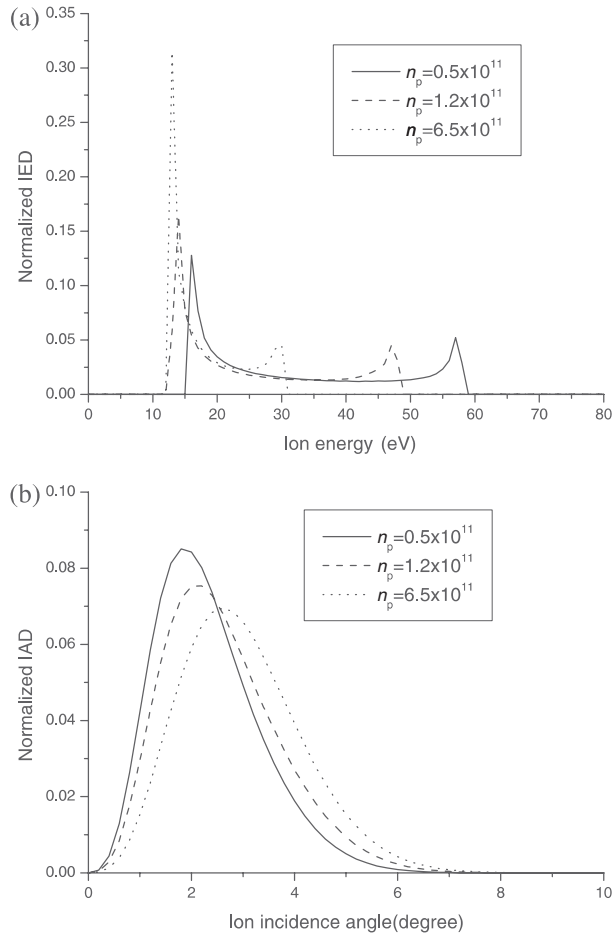

Figure 6. Effects of the plasma density on (*a*) the IED and (*b*) the IAD impinging on the electrode. The applied rf frequency, the rf-bias power and the ion temperature are 13.56 MHz, 75 W and 300 K, respectively.

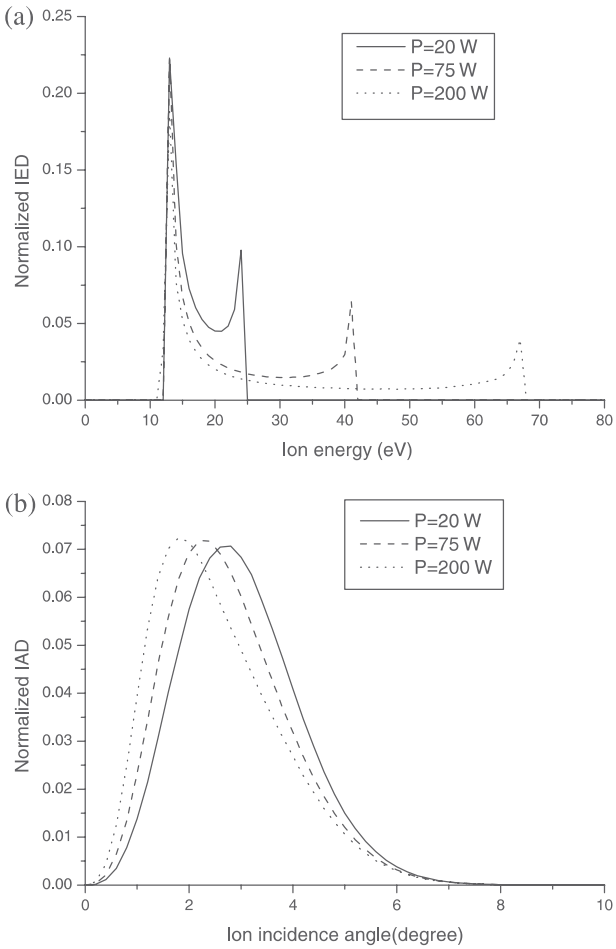

Figure 7. Effects of the rf-bias power on (*a*) the IED and (*b*) the IAD impinging on the electrode. The applied rf frequency, the plasma density and the ion temperature are kept constant at 13.56 MHz, 2.1 $\times$ 10^{11} cm^{-3} and 300 K, respectively.

power and the plasma density are set as 1.0 MHz, 9.7 W and 3.22 $\times$ 10^{10} cm^{-3}, respectively. From figure 3(*b*), one can see that the simulated results of the sheath voltage are in agreement with the experimental ones [12] in figure 3(*a*). Therefore, it is considered that our numerical results may predict the measured sheath voltage.

Figures 4(*a*) and (*b*) show the voltage amplitude at the electrode and the corresponding time dependent sheath width for rf-bias frequency values from 3.82 to 76.25 MHz. One can see that the potential amplitude at the electrode and the sheath width decrease with increasing rf frequency any time in a rf cycle. As the potential reaches its maximum voltage drop in one rf cycle, the sheath width also reaches its maximum.

The effects of the rf frequency on the IED and IAD at the electrode are shown in figure 5 while keeping the rf-bias power and the plasma density at their base values. In figure 5(*a*), the energy separation between the low and high energy peaks becomes narrower with increasing rf frequency, and the IED shows almost a single peak for the rf-bias frequency of 76.25 MHz. The peak-to-peak voltage decreases with increasing rf frequency and this may account for the energy peak shift in the IED. When the rf frequency is low (i.e. 3.82 MHz), an ion traverses the sheath before the voltage drop changes significantly and, therefore, impinges on the electrode with an energy equal to the instantaneous voltage across the sheath when it enters the sheath. In contrast, for the high rf limit, ions will arrive at the electrode taking many rf cycles and may no longer respond to the instantaneous voltage drop across the sheath.

In figure 5(*b*), the ion angles impinging on the electrode are within 8°. We note that as the rf frequency is increased, the IAD becomes thinner. However, the ion number of the incidence angle between 2° and 3.5° increases, and the position of the ion angle peak shifts a little to the large angle regime. The increasing rf frequency shifts the high energy peak position of the IED to the lower energy regime while the low one to the higher energy regime. Thus, according to the definition of the ion incident angle, the shift of the IAD can be explained by the variation in the ion energy (or velocity), though this shift is not very sharp.

Finally, figures 6 and 7 show the variation of the IED and IAD during one rf cycle for different plasma densities and rf-bias powers, respectively. The simulated results of IEDs in figures 6(*a*) and 7(*a*) are consistent with those given by Edelberg and Aydil [7]. The ion angles impinging on the electrode are small ones. The peak width of the IAD in figure 6(*b*) does not change significantly for different ion densities, just like that in figure 7(*b*) for different rf-bias

powers. The locations of the ion angular peaks in figure 6(*b*) shift a little to the large angle regime while the heights of the ion angle peaks drop with increase in the plasma density. The peak locations of the IAD in figure 7(*b*) shift a little to the small angle regime but the heights of the peaks for ions do not change obviously as the rf-bias power increases.

Thus, in order to obtain a higher etching rate and better ion anisotropy at the electrode (target), the small angle distribution of the ion impinging on the electrode could be obtained by increasing the applied rf frequency or rf-bias power. In addition, as shown in figure 6(*b*), the ion incident angles at the electrode are affected by changes in the plasma density.

4. Conclusion

For the collisionless rf plasma sheath, a self-consistent fluid model is used to study the ion transport characteristics across the sheath, and a simplified Monte Carlo method is applied to calculate the angular distribution of the ions impinging on the electrode. We present the spatiotemporal variations of the voltage amplitude, the ion density and the electron density inside the sheath. Furthermore, we study the effects of various rf frequencies on the voltage at the electrode, the sheath width, the IED and IAD impinging on the rf-biased electrode. It is found that the IED at the electrode merges into a single peak when the rf frequency increases. The incident angles of ions impinging on the electrode are small angles of less than 8° and the IAD becomes narrower with increase in the rf frequency. The ion energy and angular distributions are affected by changes in plasma densities and rf-bias powers. Therefore, plasma etching anisotropy can be improved by increasing the rf frequency or rf-bias power. However, the incident angles of ions arriving at the electrode move to the large angle regime when increasing the plasma density.

References

[1] Oksuz L and Hershkowitz N 2002 *Phys. Rev. Lett.* **89** 145001
[2] Liu Y H, Liu Z L, Yao K L, Liu H X and Wang J Z 2000 *J. Phys. D: Appl. Phys.* **33** 812
[3] Wei H L, Liu Z L and Yao K L 2000 *Vacuum* **57** 87
[4] Edelberg E A, Perry A J, Benjamin N and Aydil E S 1999 *J. Vac. Sci. Technol.* A **17** 506
[5] Lieberman M A 1988 *IEEE Trans. Plasma Sci.* **16** 638
[6] Lieberman M A 1989 *IEEE Trans. Plasma Sci.* **17** 338
[7] Edelberg E A and Aydil E S 1999 *J. Appl. Phys.* **86** 4799
[8] Dai Z L, Wang Y N and Ma T C 2002 *Phys. Rev.* E **65** 136403
[9] Kawamura E, Vahedi V, Lieberman M A and Birdsall C K 1999 *Plasma Sources Sci. Technol.* **8** R45
[10] Raja L L and Linne M 2002 *J. Appl. Phys.* **92** 7032
[11] Gottscho R A 1993 *J. Vac. Sci. Technol.* B **11** 1884
[12] Sobolewski M A 1999 *Phys. Rev.* E **59** 1059